J. Fluid Mech. (2021), *vol*. 927, A36, doi:10.1017/jfm.2021.782

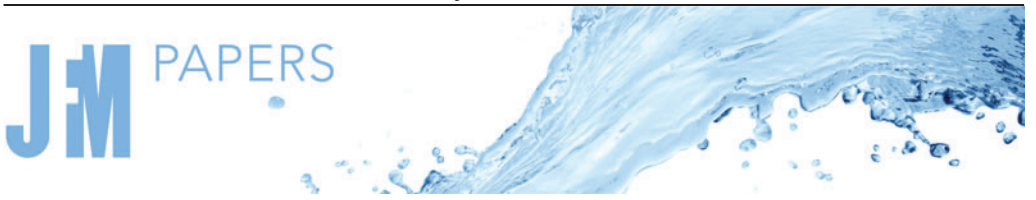

Linear stability analysis of a Newtonian ferrofluid cylinder surrounded by a Newtonian fluid

Romain Canu[1] **and Marie-Charlotte Renoult**[1],†

[1]Normandie Univ, UNIROUEN, INSA Rouen, CNRS, CORIA, 76000 Rouen, France

(Received 19 May 2021; revised 30 July 2021; accepted 30 August 2021)

We performed a linear stability analysis of a Newtonian ferrofluid cylinder surrounded by a Newtonian non-magnetic fluid in an azimuthal magnetic field. A wire is used at the centre of the ferrofluid cylinder to create this magnetic field. Isothermal conditions are considered and gravity is ignored. An axisymmetric perturbation is imposed at the interface between the two fluids and a dispersion relation is obtained allowing us to predict whether the flow is stable or unstable with respect to this perturbation. This relation is dependent on the Ohnesorge number of the ferrofluid, the dynamic viscosity ratio, the density ratio, the magnetic Bond number, the relative magnetic permeability and the dimensionless wire radius. Solutions to this dispersion relation are compared with experimental data from Arkhipenko *et al.* (*Fluid Dyn.*, vol. 15, issue 4, 1981, pp. 477–481) and, more recently, Bourdin *et al.* (*Phys. Rev. Lett.*, vol. 104, issue 9, 2010, 094502). A better agreement than the inviscid theory and the theory that only takes into account the viscosity of the ferrofluid is shown with the data of Arkhipenko *et al.* (*Fluid Dyn.*, vol. 15, issue 4, 1981, pp. 477–481) and those of Bourdin *et al.* (*Phys. Rev. Lett.*, vol. 104, issue 9, 2010, 094502) for small wavenumbers.

Key words: magnetic fluids

1. Introduction

Ferrofluids are superparamagnetic suspensions comprised of nanometric magnetic particles in a water- or oil-based liquid. A surfactant is used to prevent the agglomeration of particles. Given the nanometric size of the particles, ferrofluids can be considered as a single liquid phase. Due to the ability to control them with magnetic fields, ferrofluids are of interest in various flows such as liquid jets. During jet atomisation, cylindrical ligament structures are observed. Thus, it is interesting to study the stability of a ferrofluid cylinder

† Email address for correspondence: renoultm@coria.fr

under a magnetic field. Few experiments have been conducted on ferrofluid cylinders as of now, nevertheless data have been collected. Arkhipenko *et al.* (1981) studied the stability of a ferrofluid cylinder in glycerine subjected to an azimuthal magnetic field created by a cylindrical conductor inside the ferrofluid. The cylinder was initially stabilised with a high magnetic field intensity and then destabilised by decreasing this intensity. The growth rate and the wavelength of the fastest growing mode at different magnetic field intensities were measured. Bourdin, Bacri & Falcon (2010) performed a similar experiment using Freon instead of glycerine as the surrounding fluid. Contrary to Arkhipenko *et al.* (1981), their measurements were only made at high magnetic field intensities when the cylinder was stable. The perturbation frequency was imposed at one location and the associated wavenumber was measured. The theoretical models based on a linear stability analysis developed to date tend to overpredict the experimental data. Considering an inviscid ferrofluid with an inviscid surrounding fluid (Arkhipenko *et al.* 1981), the predicted growth rate is between 3 and 15 times higher than that observed in experiments. By considering the ferrofluid viscosity, but neglecting the surrounding fluid (Canu & Renoult 2021), this error decreases, although the growth rate is still 2 to 7 times higher than the experimental data. Regarding the difference with the experimental data of Bourdin *et al.* (2010), the inviscid theory used by the authors (theory of Arkhipenko *et al.* (1981) but without considering the radius of the cylindrical conductor and the density of the surrounding fluid) has a relative error of around 40 %–50 %, whereas that of the viscous theory without surrounding fluid (Canu & Renoult 2021) is around 20 %–30 %. In the case of these two experiments the difference may be explained by the viscosity of the surrounding fluid, which is not negligible, especially for the case of the Arkhipenko *et al.* (1981) experiments. Therefore, there is a need to consider the surrounding fluid viscosity in stability analysis. This addition will bring us closer to experimental conditions that can be encountered in medicine, for example, where a ferrofluid can be injected into a viscous biological liquid for drug targeting applications.

In the literature, several studies have theoretically considered a viscous fluid surrounded by another viscous fluid in a non-magnetic case. The first linear stability analysis was conducted by Tomotika (1935). He considered a cylinder of a viscous Newtonian fluid surrounded by an infinite Newtonian fluid. He obtained a general dispersion relation under the form of a determinant and solved it by considering a negligible inertia compared with the viscous effects. In another study, Tomotika (1936) investigated the same configuration but with the cylinder placed in an extending velocity field where the radial and axial components are respectively proportional to the radial and axial coordinates. In this type of field, the cylinder remains cylindrical until it breaks up into small drops once it becomes very thin. Studies on cylinders placed in extending velocity fields were also conducted by Mikami, Cox & Mason (1975), who performed experimental measurements in addition to theoretical analyses, and by Khakhar & Ottino (1987). Kinoshita, Teng & Masutani (1994) analysed the same case as Tomotika (1935). Similarly, they ignored inertia and considered Stokes flows but, contrary to Tomotika (1935), they obtained an explicit dispersion relation. They also obtained simplified dispersion relations for limiting cases and found that the density ratio, the viscosity ratio (density and viscosity of the outer fluid compared with the inner fluid) and the Ohnesorge number tend to stabilise the jet when they are large. Furthermore, they observed that the density ratio is only significant for gases surrounded by liquids. Stone & Brenner (1996) also simplified the dispersion relation for the case in which both fluids have the same viscosity and then generalised the results for several concentric fluids. In previous studies, velocity has been expressed with a Stokes streamfunction. Funada & Joseph (2002) compared three methods: velocity

expressed with a Stokes streamfunction while considering viscosity; velocity expressed with a potential while considering viscosity; and velocity expressed with a potential while ignoring viscosity. The authors found that the three methods converge for sufficiently high Reynolds numbers and that the second method gives intermediate results for low Reynolds numbers. Gunawan, Molenaar & van de Ven (2002) explored the stability of two proximate cylinders immersed in another fluid. In this case, the breakup of the cylinders accelerates when the viscosity ratio is high and the distance between the cylinders is short. Furthermore, according to the values of the viscosity ratio and the distance between the cylinders, the deformations of the cylinders will occur in or out of phase. In the literature, other kinds of viscous fluids were also studied. Gadkari & Thaokar (2013) regarded conductive fluids placed in an axial or radial electric field as well as the influence of this field on asymmetric modes of the perturbation. Finally, Patrascu & Balan (2018) analysed the stability of viscoelastic fluids immersed in another viscoelastic fluid and compared them with the limiting cases in which the fluids are Newtonian.

Regarding the magnetic case, there is the work of Korovin in which a ferrofluid cylinder is surrounded by another ferrofluid with different magnetic permeability and same density. In Korovin (2001), an axial magnetic field is applied and the two ferrofluids have a different viscosity. For this case, an explicit dispersion relation was obtained for the particular case where the viscous forces are dominant. Then, the case in which both ferrofluids have the same viscosity was treated (Korovin 2002; Kazhan & Korovin 2003). This time, the dispersion relation was obtained using a single equation of motion valid for both ferrofluids and at the interface. The same methodology was used in Korovin (2004) but for the case of an azimuthal magnetic field created by a cylindrical conductor placed at the centre of the inner ferrofluid. Again, both ferrofluids have the same density and viscosity. In a recent paper (Korovin 2020), for the case of an inviscid ferrofluid without surrounding fluid, a Langevin law for the magnetisation of the ferrofluid was considered instead of a linear magnetisation usually assumed.

In this work, we will perform a linear stability analysis of a Newtonian ferrofluid surrounded by a Newtonian non-magnetic fluid in an azimuthal magnetic field, for the general case where the two fluids have different densities and viscosities. After formulating this problem with different assumptions, we will derive the bulk equations for both fluids and the jump conditions across the interface between them. A general dispersion relation in explicit form will then be obtained, providing another formulation of this relation compared with previous studies. Its solutions will finally be compared with the experimental data (Arkhipenko *et al.* 1981; Bourdin *et al.* 2010).

2. Formulation

We consider an incompressible Newtonian ferrofluid cylinder of infinite length surrounded by a Newtonian non-magnetic fluid. The system is placed in a steady axisymmetric azimuthal magnetic field. Isothermal conditions are also assumed and gravity is ignored. According to Canu & Renoult (2021), under these assumptions, the azimuthal magnetic field should be in the form $\boldsymbol{H} = B/r\boldsymbol{e_\theta}$ with B a constant, r the radial distance and e_θ the azimuthal unit vector. A wire with radius R_w is used at the centre of the ferrofluid cylinder to create this magnetic field by passing an electric current of intensity I through it. A representation of this configuration is shown in figure 1. Considering an infinite length wire and a uniform electrical current inside it, the created magnetic field is such that $B = I/2\pi$. In the basic state, both fluids are considered at rest. This state is perturbed by imposing a small-amplitude axisymmetric disturbance. Linear stability

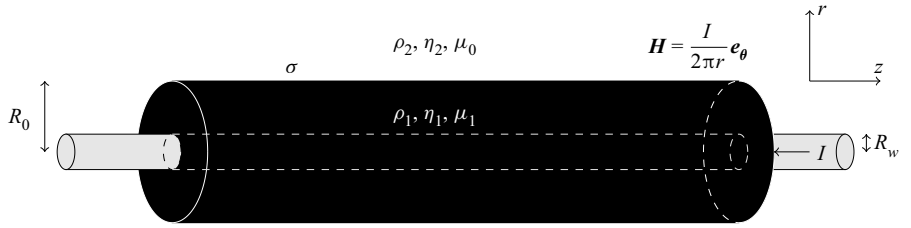

Figure 1. Representation of a Newtonian ferrofluid cylinder around a wire and surrounded by a Newtonian non-magnetic fluid.

analysis is then performed to investigate whether the flow is stable or unstable with respect to this disturbance. The governing equations of this flow are described below.

3. Governing equations

The equations, valid for both the ferrofluid and the surrounding fluid, are presented below. The mass and momentum balance equations can be expressed as follows:

$$\boldsymbol{\nabla} \cdot \boldsymbol{U_i} = 0, \tag{3.1}$$

$$\rho_i \left(\frac{\partial \boldsymbol{U_i}}{\partial t} + \boldsymbol{U_i} \cdot \boldsymbol{\nabla} \boldsymbol{U_i} \right) = -\boldsymbol{\nabla} \Pi_i + \boldsymbol{\nabla} \cdot \tau_i, \tag{3.2}$$

with $\boldsymbol{U_i}$ the velocity, ρ_i the density, $\tau_i = \eta_i(\boldsymbol{\nabla} \boldsymbol{U_i} + \boldsymbol{\nabla} \boldsymbol{U_i^t})$ the viscous stress tensor, η_i the dynamic viscosity and Π_i defined by $\Pi_i = P_i + P_{si}$, where P_i refers to thermodynamic pressure and $P_{si} = \mu_0 \int_0^H \upsilon_i (\partial M_i / \partial \upsilon_i)\, \mathrm{d}H$ to magnetostrictive pressure. In this last term, μ_0 is the permeability of free space, υ_i the specific volume, and M_i the magnetisation. The subscript i takes the value 1 for the ferrofluid and 2 for the surrounding fluid. In particular, $M_2 = 0$ and $\Pi_2 = P_2$.

As neither fluid is electrically conductive, Maxwell's equations are thus

$$\boldsymbol{\nabla} \cdot \boldsymbol{B_i} = 0, \tag{3.3}$$

$$\boldsymbol{\nabla} \times \boldsymbol{H_i} = \boldsymbol{0}, \tag{3.4}$$

with $\boldsymbol{B_i}$ the magnetic induction field, which can be expressed as

$$\boldsymbol{B_i} = \mu_0 \left(\boldsymbol{H_i} + \boldsymbol{M_i} \right) = \mu_i \boldsymbol{H_i}, \tag{3.5}$$

with μ_i the magnetic permeability of the fluid. For a ferrofluid, the magnetisation follows a Langevin law (see e.g. Korovin 2020). Nevertheless, for sufficiently weak magnetic fields, the response of the ferrofluid can be considered as linear, homogeneous and isotropic. The magnetic field intensities encountered in this paper satisfy this condition. The magnetic permeability of the ferrofluid μ_1 can therefore be assumed constant. For the non-magnetic surrounding fluid, $\mu_2 = \mu_0$.

For the jump conditions across the interface, the unit normal vector is introduced. It is defined at a point on the interface, pointing from the ferrofluid to the surrounding fluid, and is given by $\boldsymbol{n} = \boldsymbol{\nabla} S / ||\boldsymbol{\nabla} S|| = 1/\sqrt{1 + (\partial r_s/\partial z)^2}\boldsymbol{e_r} - (\partial r_s/\partial z)/\sqrt{1 + (\partial r_s/\partial z)^2}\boldsymbol{e_z}$, where $S = r - r_s$ is introduced to localise the position of the interface $S = 0$. The first jump

condition is obtained by writing the mass balance equation at the interface without mass exchange between the two phases

$$\boldsymbol{U_i} \cdot \boldsymbol{n} = -\frac{1}{||\nabla S||}\frac{\partial S}{\partial t} \quad \text{at } r = r_s. \tag{3.6}$$

Moreover, the same assumption as in Tomotika (1935) is considered, namely no slip at the interface leading to

$$[\boldsymbol{U} \times \boldsymbol{n}] = \boldsymbol{0} \quad \text{at } r = r_s, \tag{3.7}$$

with the convention $[A] = A_2 - A_1$. Both (3.6) and (3.7) lead to the continuity of the velocity components across the interface. Regarding the jump conditions for momentum, there is continuity in the tangential component of the stress acting on the interface

$$[(\boldsymbol{n} \cdot \boldsymbol{T}) \times \boldsymbol{n}] = \boldsymbol{0} \quad \text{at } r = r_s, \tag{3.8}$$

with $\boldsymbol{T}$ the stress tensor such that $\boldsymbol{T_i} = -(P_i^* + (1/2)\mu_0 H_i^2)\boldsymbol{I} + \boldsymbol{B_i H_i} + \tau_i$, $\boldsymbol{I}$ the identity matrix, $P_i^* = \Pi_i + P_{mi}$ and $P_{mi} = \mu_0 \int_0^H M_i \, \mathrm{d}H$ the magnetic pressure. The jump of the normal component of the stress acting on the interface involves surface tension

$$[(\boldsymbol{n} \cdot \boldsymbol{T}) \cdot \boldsymbol{n}] = \sigma\kappa \quad \text{at } r = r_s, \tag{3.9}$$

with $\kappa = \nabla \cdot \boldsymbol{n}$ the curvature which is twice the mean curvature.

The jump conditions for the magnetic field imply the continuity of the normal component of $\boldsymbol{B}$ and the tangential component of $\boldsymbol{H}$ across the interface. Replacing $\boldsymbol{B}$ by expression (3.5), one finds

$$\mu_1 \boldsymbol{H_1} \cdot \boldsymbol{n} = \mu_0 \boldsymbol{H_2} \cdot \boldsymbol{n} \quad \text{at } r = r_s, \tag{3.10}$$

$$\boldsymbol{H_1} \times \boldsymbol{n} = \boldsymbol{H_2} \times \boldsymbol{n} \quad \text{at } r = r_s. \tag{3.11}$$

By using $\boldsymbol{n} \cdot \boldsymbol{I} \times \boldsymbol{n} = \boldsymbol{0}$ as well as (3.5), (3.10) and (3.11), (3.8) and (3.9) are thus reduced to

$$(\boldsymbol{n} \cdot \tau_1) \times \boldsymbol{n} - (\boldsymbol{n} \cdot \tau_2) \times \boldsymbol{n} = \boldsymbol{0} \quad \text{at } r = r_s, \tag{3.12}$$

$$P_1^* + P_n - (\boldsymbol{n} \cdot \tau_1) \cdot \boldsymbol{n} = P_2 - (\boldsymbol{n} \cdot \tau_2) \cdot \boldsymbol{n} + \sigma \nabla \cdot \boldsymbol{n} \quad \text{at } r = r_s, \tag{3.13}$$

with $P_n = (1/2)\mu_0 M_{1n}^2$; the n index refers to the normal component.

The bulk equations (3.1)–(3.2) as well as the jump conditions across the interface (3.6), (3.10)–(3.13) are made dimensionless using the Rayleigh time $\sqrt{\rho_1 R_0^3/\sigma}$, R_0, σ/R_0, an arbitrary magnetic field intensity H_0 and μ_0 as the characteristic time, length, pressure, magnetic field and magnetic permeability, respectively. The characteristic scales of the Rayleigh problem are chosen to enable the comparison of solutions with a magnetic field to those of the non-magnetic problem.

The basic state, denoted by subscript 0 such that Π_{0i} is the basic state of Π_i for example, is obtained by taking $\boldsymbol{H_{01}} = 1/r\boldsymbol{e_\theta}$ and $\boldsymbol{U_{0i}} = \boldsymbol{0}$ in the equations. It is found that Π_{01} and P_{02} are constants that are linked in the following way:

$$\Pi_{01} + \tfrac{1}{2}N_{Bo,m} = P_{02} + 1 \quad \text{at } r = 1, \tag{3.14}$$

with $N_{Bo,m} = \mu_0(\mu_r - 1)H_0^2R_0/\sigma$ the magnetic Bond number, and $\mu_r = \mu_1/\mu_0$ the relative permeability; $N_{Bo,m}$ can be expressed as the product of two numbers $(\mu_r - 1)$ and $\Gamma_m = \mu_0 H_0^2 R_0/\sigma$, with Γ_m a magnetic parameter that does not depend on μ_r.

The induced flow is decomposed around the basic state, as follows: $\boldsymbol{U_i} = \boldsymbol{u_i}$, $\Pi_i = \Pi_{0i} + \pi_i$, $\boldsymbol{H_i} = \boldsymbol{H_{0i}} + \boldsymbol{h_i}$ and $r_s = 1 + \zeta$ with $\boldsymbol{u_i}$, π_i, $\boldsymbol{h_i}$ the perturbed quantities in phase i and ζ the surface perturbation. The dimensionless equations are linearised, and we thus obtain the equations for the perturbed quantities

$$\frac{1}{r}\frac{\partial r u_{ir}}{\partial r} + \frac{\partial u_{iz}}{\partial z} = 0, \tag{3.15}$$

$$\frac{\partial u_{1r}}{\partial t} + \frac{\partial \pi_1}{\partial r} - Oh_1\left(\frac{1}{r}\frac{\partial^2 r u_{1r}}{\partial r^2} - \frac{1}{r^2}\frac{\partial r u_{1r}}{\partial r} + \frac{\partial^2 u_{1r}}{\partial z^2}\right) = 0, \tag{3.16}$$

$$\rho_r\frac{\partial u_{2r}}{\partial t} + \frac{\partial P_2}{\partial r} - Oh_1\eta_r\left(\frac{1}{r}\frac{\partial^2 r u_{2r}}{\partial r^2} - \frac{1}{r^2}\frac{\partial r u_{2r}}{\partial r} + \frac{\partial^2 u_{2r}}{\partial z^2}\right) = 0, \tag{3.17}$$

$$\frac{\partial u_{1z}}{\partial t} + \frac{\partial \pi_1}{\partial z} - Oh_1\left(\frac{1}{r}\frac{\partial r\dfrac{\partial u_{1z}}{\partial r}}{\partial r} + \frac{\partial^2 u_{1z}}{\partial z^2}\right) = 0, \tag{3.18}$$

$$\rho_r\frac{\partial u_{2z}}{\partial t} + \frac{\partial P_2}{\partial z} - Oh_1\eta_r\left(\frac{1}{r}\frac{\partial r\dfrac{\partial u_{2z}}{\partial r}}{\partial r} + \frac{\partial^2 u_{2z}}{\partial z^2}\right) = 0, \tag{3.19}$$

$$u_{ir} - \frac{\partial \zeta}{\partial t} = 0 \quad \text{at } r = 1, \tag{3.20}$$

$$\frac{\partial u_{1r}}{\partial z} + \frac{\partial u_{1z}}{\partial r} - \eta_r\left(\frac{\partial u_{2r}}{\partial z} + \frac{\partial u_{2z}}{\partial r}\right) = 0 \quad \text{at } r = 1, \tag{3.21}$$

$$\pi_1 - N_{Bo,m}\zeta - 2Oh_1\frac{\partial u_{1r}}{\partial r} + 2Oh_1\eta_r\frac{\partial u_{2r}}{\partial r} - p_2 + \zeta + \frac{\partial^2 \zeta}{\partial z^2} = 0 \quad \text{at } r = 1, \tag{3.22}$$

$$\mu_r h_{1r} - h_{2r} = 0 \quad \text{at } r = 1, \tag{3.23}$$

$$h_{1z} - h_{2z} = 0 \quad \text{at } r = 1, \tag{3.24}$$

$$h_{1\theta} - h_{2\theta} = 0 \quad \text{at } r = 1, \tag{3.25}$$

with $Oh_1 = \eta_1/\sqrt{\rho_1\sigma R_0}$, the Ohnesorge number of the ferrofluid, $\rho_r = \rho_2/\rho_1$ the density ratio and $\eta_r = \eta_2/\eta_1$ the dynamic viscosity ratio. Furthermore, due to (3.3) and (3.4), the perturbation of the magnetic fields $\boldsymbol{h_i}$ are curl- and divergence-free.

The system of equations is linear with respect to t and z, and nonlinear with respect to r. Hence, we seek solutions in the form $A(r)\exp(\mathrm{i}kz + \alpha t)$, where $A(r)$ is an unknown function of r. Since this study explores temporal stability, we take k to be real,

and $\alpha = \alpha_r + \mathrm{i}\alpha_i$ to be complex, such that k, α_r and α_i are respectively the wavenumber, growth rate and oscillation frequency of the perturbation. Due to the azimuthal shape of the magnetic field, the perturbation $\boldsymbol{h_i}$ is decoupled from the other equations. Equations (3.23)–(3.25) are therefore not required to obtain the dispersion relation.

4. Dispersion relation

Due to the incompressibility assumptions, the velocity in each fluid can be expressed using a Stokes streamfunction ψ such that $u_{ir} = -(1/r)(\partial\psi_i/\partial z)$ and $u_{iz} = (1/r)(\partial\psi_i/\partial r)$. Moreover, the magnetic field is curl-free inside each fluid and can be written as a gradient of a magnetic scalar potential ϕ such that $\boldsymbol{h_i} = -\boldsymbol{\nabla}\phi_i$. Because the perturbation of the magnetic field is also divergence-free in each fluid, we have

$$\Delta\phi_i = 0. \tag{4.1}$$

No slip and no penetration are considered at the wire surface and there is no perturbation of the magnetic field at this location. These boundary conditions are expressed by

$$-\frac{1}{r}\frac{\partial\psi_1}{\partial z} = 0 \quad \text{and} \quad \frac{1}{r}\frac{\partial\psi_1}{\partial r} = 0 \quad \text{at } r = \delta_w, \tag{4.2}$$

$$\phi_1 = 0 \quad \text{at } r = \delta_w, \tag{4.3}$$

with $\delta_w = R_w/R_0$ the dimensionless wire radius. Equations (3.23)–(3.25) and (4.1) lead to $\phi_i = 0$ showing that, for an azimuthal magnetic field, there is no axisymmetric perturbation of the magnetic field. The previous system of (3.15)–(3.22) is solved using the same method as in Canu & Renoult (2021), with the following dispersion relation being obtained:

$$\begin{aligned}
&\alpha^2 + \alpha^2\rho_r\frac{\hat{b}_2 K_0(k)}{I_0(k) - \hat{b}_1 K_0(k)} + 2Oh_1\alpha k \\
&\quad\left[\frac{kI_0(k) - I_1(k) + \check{a}_1\left(l_1 I_0(l_1) - I_1(l_1)\right) - \hat{b}_1\left(kK_0(k) + K_1(k)\right) - \check{b}_1\left(l_1 K_0(l_1) + K_1(l_1)\right)}{I_0(k) - \hat{b}_1 K_0(k)}\right. \\
&\quad\left.+\eta_r\frac{\hat{b}_2\left(kK_0(k) + K_1(k)\right) + \check{b}_2\left(l_2 K_0(l_2) + K_1(l_2)\right)}{I_0(k) - \hat{b}_1 K_0(k)}\right] \\
&\quad - k\left(1 - k^2 - N_{Bo,m}\right)\left[\frac{I_1(k) + \check{a}_1 I_1(l_1) + \hat{b}_1 K_1(k) + \check{b}_1 K_1(l_1)}{I_0(k) - \hat{b}_1 K_0(k)}\right] = 0.
\end{aligned} \tag{4.4}$$

In this relation, I_0, I_1, K_0 and K_1 are the modified Bessel functions of the first and second kinds at the orders 0 and 1, l_i is a modified wavenumber for fluid i such that $l_1^2 = k^2 + (\alpha/Oh_1)$ and $l_2^2 = k^2 + (\alpha\rho_r/Oh_1\eta_r)$. The other quantities $\check{a}_1$, $\hat{b}_1$, $\check{b}_1$, $\hat{b}_2$ and $\check{b}_2$ are coefficients defined in Appendix A and are explicitly dependent on k, l_1, l_2, η_r and δ_w. Here, the dispersion relation has a general explicit form. It tends towards the non-magnetic case of Tomotika (1935), obtained under a determinant form, for $N_{Bo,m} = 0$ and $\delta_w \to 0$. We also retrieve the dispersion relation of Korovin (2004) by taking $\rho_r = 1$, $\eta_r = 1$ and considering a non-magnetic surrounding fluid. As with the azimuthal case in Canu &

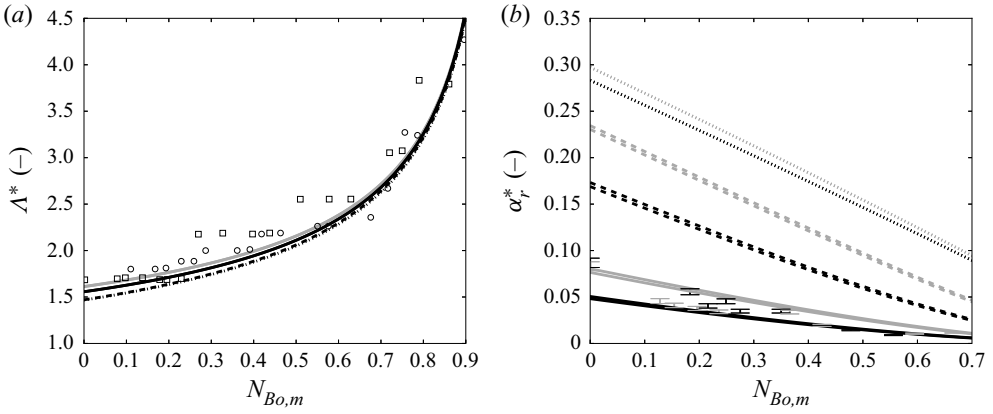

Figure 2. Comparison with the experimental data of Arkhipenko *et al.* (1981) in an azimuthal magnetic field. (*a*) Value of Λ^* as a function of $N_{Bo,m}$: □, experimental data with a column of 18 cm; ◯, experimental data with a column of 50 cm. (*b*) Value of α_r^* as a function of $N_{Bo,m}$; error bars correspond to the experimental data and derive from a lack of information regarding the ferrofluids used. Both: dotted lines correspond to the inviscid theory of Arkhipenko *et al.* (1981); dashed lines to the viscous theory without surrounding fluid of Canu & Renoult (2021); and solid lines to the present viscous theory with surrounding fluid. Black corresponds to $R_0 = 2.1$ mm and grey to $R_0 = 2.8$ mm. Identical lines are plotted for two ferrofluids FF1 and FF2 from table 1.

Renoult (2021), the cutoff wavenumber only depends on $N_{Bo,m}$, with the cylinder being stable for all wavenumbers when $N_{Bo,m} > 1$. This relation is solved and compared below with experimental results taken from the literature.

5. Comparison with experimental data

The dispersion relation (4.4) is a transcendental equation due to the modified Bessel functions that depend on α through l_1 and l_2. To solve this equation, the method of Luck, Zdaniuk & Cho (2015) is used. The resulting solutions are then compared with experimental data and previous theoretical studies. In figure 2, the wavelength (divided by 2π) $\Lambda^* = 1/k^*$ and the growth rate α_r^* of the most unstable mode are plotted as a function of $N_{Bo,m}$ and compared with the experiment of Arkhipenko *et al.* (1981). Note that α_r^* is dimensionless here contrary to the data given in Arkhipenko *et al.* (1981). In their experiment, a ferrofluid cylinder is around a cylindrical conductor and is surrounded by glycerine. The conductor has a fixed radius ($R_w = 1$ mm) whereas the one of the ferrofluid cylinder varies. Arkhipenko *et al.* (1981) realised the wavelength measurements for two conductor lengths (18 and 50 cm) without indication on the radius of the ferrofluid cylinder. For the growth rate measurements, two data sets are provided for two cylinder radii ($R_0 = 2.1$ and $R_0 = 2.8$ mm). In their paper, two ferrofluids are mentioned. However, for both measurements, no indication is provided on the ferrofluid used. Ferrofluid properties are shown in table 1 and $\rho_r = 1$ and $\eta_r = 28.3$ are chosen here for the density and viscosity of the surrounding fluid (glycerine) compared with those of the ferrofluid, as indicated in Arkhipenko *et al.* (1981). In a previous study (Canu & Renoult 2021), we showed that taking into account the ferrofluid viscosity without the surrounding fluid better predicts the growth rate compared with the inviscid theory of Arkhipenko *et al.* (1981). However, the difference with the experimental data was still significant, probably due to the viscosity of the surrounding fluid being ignored. Indeed, the latter is approximately 30 times higher than those of the ferrofluid, and thus its effect

Name	Components	ρ_1 (kg m^{-3})	η_1 (kg m^{-1} s^{-1})	σ (N m^{-1})	μ_r (–)
FF1	kerosene + magnetite + oleic acid	1220	6×10^{-3}	9.2×10^{-3} (with glycerine)	2.2
FF2	kerosene + magnetite + oleic acid	1157	6×10^{-3}	1.1×10^{-2} (with glycerine)	3.5
FF3	water + maghemite + unknown surfactant	1534	1.4×10^{-3}	5.5×10^{-3} (with Freon)	1.75

Table 1. Ferrofluid properties under standard laboratory conditions taken from Arkhipenko *et al.* (1981) (for FF1 and FF2) and Bourdin *et al.* (2010) (for FF3).

cannot be ignored. With the present theory, the predicted growth rate is very close to the experimental data, especially for larger values of $N_{Bo,m}$. For the case with $R_0 = 2.1$ mm, the relative error is between 2.7 % and 47 % with a mean of approximately 28 %. For $R_0 = 2.8$ mm, the relative error is between 0.3 % and 88 % with a mean varying from 31 % to 51 % depending on the ferrofluid used. The uncertainty regarding the ferrofluid used in the experiment does not lead to a better estimation of the error. Indeed, to make dimensionless the experimental values of Arkhipenko *et al.* (1981), the Rayleigh time is used. This time depends on the density and the surface tension which are different for the ferrofluid FF1 and FF2 (table 1). This uncertainty is represented by error bars in figure 2. The range of relative error given above corresponds to the extremum values between the relative errors calculated for FF1 and FF2 for all experimental data points. By contrast, the prediction for $R_0 = 2.1$ mm seems to better correspond to the experimental data for $R_0 = 2.8$ mm. On this point, the experimental data do not follow the theoretical prediction of all the models (inviscid theory, viscous theory without surrounding fluid and viscous theory with surrounding fluid) about the decrease in the growth rate for thinner layer of fluid (Canu & Renoult 2021). The possibility of a typographical error in the figure legend of Arkhipenko *et al.* (1981) cannot be discounted but further experimental data are necessary to confirm that. In this case, the relative errors would be lower than those given above. Better predictions are also observed for the most unstable wavelength. The curves for the inviscid theory and the viscous theory without surrounding fluid are almost overlapped whereas the one for the present viscous theory deviates clearly from the others. This observation shows that, for this experiment, the effect of the surrounding fluid viscosity is more significant than the one of the ferrofluid viscosity which is coherent with the fact that the surrounding fluid is almost 30 times more viscous than the ferrofluid. Furthermore, the difference between the various models is greater for lower values of $N_{Bo,m}$, because for $N_{Bo,m}$ close to 1, the unstable regime is restricted to very small wavenumbers. For these values, the effect of viscosity is indeed less visible. Another issue concerns the finite length of the ferrofluid cylinder. Side effects should occur with greater importance for the smaller cylinder producing thus a slight difference with the theoretical predictions. Moreover, the finite length of the cylinder implies that an integer number of wavelengths appears leading to the same value of wavelength for different magnetic Bond numbers and, therefore, a step profile for the experimental data instead of a continuous evolution.

The present theory is also compared with the experimental results of Bourdin *et al.* (2010) in figure 3. The same experiment as in Arkhipenko *et al.* (1981) is performed

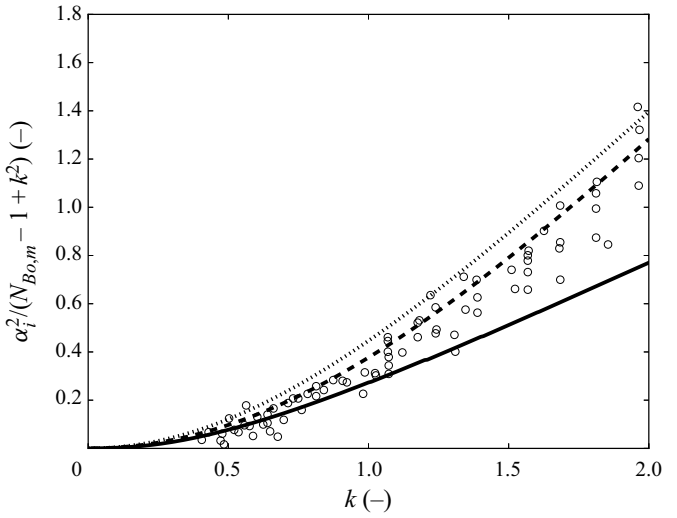

Figure 3. Comparison with the experimental data of Bourdin *et al.* (2010) in an azimuthal magnetic field. Circles correspond to experimental data for different $N_{Bo,m}$ from 1.85 to 11.57; the dotted line to the inviscid theoretical prediction made by Bourdin *et al.* (2010) (wire ignored); the dashed line to the viscous theory without surrounding fluid of Canu & Renoult (2021); and solid line to the present viscous theory with surrounding fluid plotted for the ferrofluid FF3 from table 1 and $N_{Bo,m} = 6.51$.

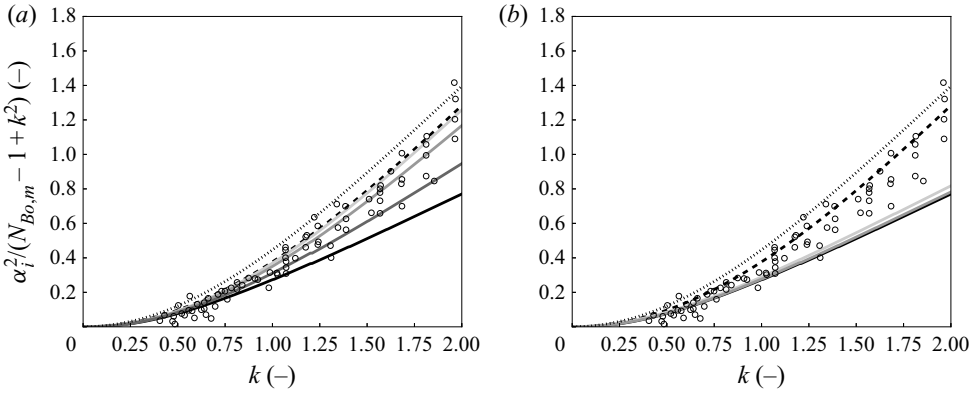

Figure 4. Comparison with the experimental data of Bourdin *et al.* (2010) in an azimuthal magnetic field. Circles correspond to experimental data for different $N_{Bo,m}$ from 1.85 to 11.57; the dotted line to the inviscid theoretical prediction made by Bourdin *et al.* (2010) (wire ignored); the dashed line to the viscous theory without surrounding fluid of Canu & Renoult (2021); and solid lines to the present viscous theory with surrounding fluid plotted for $N_{Bo,m} = 6.51$: (*a*) $\eta_r = 0.5$ and, from the darkest to the lightest, $\rho_r = 1.031$, $\rho_r = 0.5$, $\rho_r = 0.1$ and $\rho_r = 0.01$; (*b*) $\rho_r = 1.031$ and, from the darkest to the lightest, $\eta_r = 0.5$, $\eta_r = 0.25$ and $\eta_r = 0.01$.

but with Freon ($C_2Cl_3F_3$) as the surrounding fluid instead of glycerine and with another ferrofluid (FF3 in table 1). The characteristics are $\rho_r = 1.031$ and $\eta_r = 0.5$. For the viscosity of Freon, a common value is chosen because this viscosity is not provided by Bourdin *et al.* (2010). The cylindrical conductor and the initial ferrofluid cylinder

have respectively a radius of $R_w = 1.5$ and $R_0 = 3.8$ mm. Here, the cylinder is stable ($N_{Bo,m} > 1$). Therefore, the oscillation frequency of the perturbation is considered. For the theoretical predictions, only the case $N_{Bo,m} = 6.51$ is plotted, as the other cases are nearly overlapping. The present viscous theory seems to improve the prediction of the experimental data for small values of k ($k < 1$). However, for larger k values, a divergence seems to appear. The difference between the theoretical predictions with and without surrounding fluid is mainly due to the value of ρ_r. Indeed, we can see in figure 4 that, for $\rho_r \ll 1$ and fixed η_r, the results tend towards those without surrounding fluid, whereas for $\rho_r = 1.031$ and $\eta_r \ll 1$, the results are barely modified. Therefore, the effect of ρ_r seems to be more significant than the one of η_r in this experiment. However, the value of ρ_r is known in the experiment and this observation cannot explain the discrepancy between the theoretical prediction and the experimental data for large k values. New experiments would be useful to identify the source of this discrepancy.

6. Conclusions

We performed a linear stability analysis of a Newtonian ferrofluid cylinder surrounded by a Newtonian non-magnetic fluid in an azimuthal magnetic field. The cylinder was perturbed by a small-amplitude axisymmetric disturbance. We linearised the bulk equations and jump conditions and obtained a dispersion relation depending on six dimensionless parameters: the dimensionless wavenumber k, the Ohnesorge number of the ferrofluid Oh_1, the magnetic Bond number $N_{Bo,m}$, the dimensionless wire radius δ_w, the density ratio ρ_r and the viscosity ratio η_r. Solutions to this dispersion relation were compared with two experiments: the first concerns the growth rate and the wavenumber of the fastest growing mode in the unstable regime, and the second the wavenumber of an imposed perturbation frequency in the stable regime. A good agreement is observed with the experimental data of Arkhipenko *et al.* (1981), as the consideration of the viscosity of both the ferrofluid and the surrounding fluid is important for this case. Regarding the comparison with the experimental data of Bourdin *et al.* (2010), we found a good agreement for small k ($k < 1$). For larger k, a discrepancy is observed that remains for now unexplained. New experiments are thus needed to understand the cause of this discrepancy. Future studies should examine nonlinearities to predict the formation of satellite drops which are undesirable, for example, in printing field where magnetic inks can be used, and well visible in the experiments of Arkhipenko *et al.* (1981) in their figure 3.

Acknowledgements. The authors would like to thank Professor I. Mutabazi for initiating this interlaboratory project and contributing to useful discussions on its two parts.

Funding. This work was supported by LabEx EMC3 through the INFEMA (INstabilities of FErrofluid flows in MAgnetic fields) project, jointly conducted by LOMC (Normandie Univ, UNIHAVRE, CNRS) and CORIA laboratories.

Declaration of interests. The authors report no conflict of interest.

Author ORCIDs.
Marie-Charlotte Renoult https://orcid.org/0000-0003-0613-0888.

Appendix A

The dispersion relation obtained in this work is provided in a simplified form to facilitate the reading. All the notations introduced are developed below:

$$a = kI_0(k\delta_w)K_1(l_1\delta_w) + l_1I_1(k\delta_w)K_0(l_1\delta_w)$$
$$b = l_1I_0(l_1\delta_w)K_1(l_1\delta_w) + l_1I_1(l_1\delta_w)K_0(l_1\delta_w)$$
$$c = kK_0(k\delta_w)K_1(l_1\delta_w) - l_1K_1(k\delta_w)K_0(l_1\delta_w)$$
$$d = l_2I_1(k)K_1(l_1\delta_w) - l_2I_1(k\delta_w)K_1(l_1)$$
$$e = l_2K_1(k)K_1(l_1\delta_w) - l_2K_1(k\delta_w)K_1(l_1)$$
$$f = l_2I_1(l_1)K_1(l_1\delta_w) - l_2I_1(l_1\delta_w)K_1(l_1)$$
$$g = kI_0(k)K_1(l_1\delta_w) + l_1I_1(k\delta_w)K_0(l_1)$$
$$h = l_1K_1(k\delta_w)K_0(l_1) - kK_1(l_1\delta_w)K_0(k)$$
$$j = l_1I_0(l_1)K_1(l_1\delta_w) + l_1I_1(l_1\delta_w)K_0(l_1)$$
$$m = l_2K_0(l_2)K_1(k) - kK_1(l_2)K_0(k)$$
$$q = 2k^2I_1(k)K_1(l_1\delta_w) - \left(k^2 + l_1^2\right)I_1(k\delta_w)K_1(l_1)$$
$$w = 2k^2K_1(k)K_1(l_1\delta_w) - \left(k^2 + l_1^2\right)K_1(k\delta_w)K_1(l_1)$$
$$x = \left(k^2 + l_1^2\right)I_1(l_1)K_1(l_1\delta_w) - \left(k^2 + l_1^2\right)I_1(l_1\delta_w)K_1(l_1)$$
$$\gamma_1 = \left(k^2 - l_2^2\right)K_1(k)\left(K_1(l_2)\left(cg + ah\right) + K_0(l_2)\left(cd + ae\right)\right)l_2 + \left(k^2 + l_2^2\right)m\left(cd + ae\right)$$
$$\gamma_2 = \left(k^2 - l_2^2\right)K_1(k)\left(K_1(l_2)\left(cj + bh\right) + K_0(l_2)\left(cf + be\right)\right)l_2 + \left(k^2 + l_2^2\right)m\left(cf + be\right)$$
$$\breve{a}_1 = -\frac{(cq + aw)\,ml_2 - \eta_r\gamma_1}{(cx + bw)\,ml_2 - \eta_r\gamma_2}$$
$$\hat{b}_1 = \frac{a + \breve{a}_1 b}{c}$$
$$\breve{b}_1 = -\frac{cI_1(k\delta_w) + aK_1(k\delta_w) + \breve{a}_1\left(cI_1(l_1\delta_w) + bK_1(k\delta_w)\right)}{cK_1(l_1\delta_w)}$$
$$\hat{b}_2 = \frac{K_1(l_2)\left(cg + ah\right) + K_0(l_2)\left(cd + ae\right) + \breve{a}_1\left[K_1(l_2)\left(cj + bh\right) + K_0(l_2)\left(cf + be\right)\right]}{cmK_1(l_1\delta_w)}$$
$$\breve{b}_2 = \frac{\left(cd + ae\right)m - \left[K_1(l_2)\left(cg + ah\right) + K_0(l_2)\left(cd + ae\right)\right]K_1(k)l_2}{cml_2K_1(l_2)K_1(l_1\delta_w)}$$
$$+\breve{a}_1\frac{\left[\left(cf + be\right)m - \left[K_1(l_2)\left(cj + bh\right) + K_0(l_2)\left(cf + be\right)\right]K_1(k)l_2\right]}{cml_2K_1(l_2)K_1(l_1\delta_w)}.$$

References

Arkhipenko, V.I., Barkov, Yu. D., Bashtovoi, V.G. & Krakov, M.S. 1981 Investigation into the stability of a stationary cylindrical column of magnetizable liquid. *Fluid Dyn.* **15** (4), 477–481.

Bourdin, E., Bacri, J.-C. & Falcon, E. 2010 Observation of axisymmetric solitary waves on the surface of a ferrofluid. *Phys. Rev. Lett.* **104** (9), 094502.

Canu, R. & Renoult, M.-C. 2021 Linear stability analysis of a Newtonian ferrofluid cylinder under a magnetic field. *J. Fluid Mech.* **915**, A137.

Funada, T. & Joseph, D.D. 2002 Viscous potential flow analysis of capillary instability. *Intl J. Multiphase Flow* **28** (9), 1459–1478.

GADKARI, S. & THAOKAR, R. 2013 Stability of immersed viscous liquid threads under electric field. *Intl J. Engng Sci.* **62**, 9–21.

GUNAWAN, A.Y., MOLENAAR, J. & VAN DE VEN, A.A.F. 2002 In-phase and out-of-phase break-up of two immersed liquid threads under influence of surface tension. *Eur. J. Mech. (*B*/Fluids)* **21** (4), 399–412.

KAZHAN, V.A. & KOROVIN, V.M. 2003 Capillary instability of a cylindrical interface of viscous magnetic and nonmagnetic fluids subjected to an axial magnetic field. *J. Magn. Magn. Mater.* **260** (1), 222–230.

KHAKHAR, D.V. & OTTINO, J.M. 1987 Breakup of liquid threads in linear flows. *Intl J. Multiphase Flow* **13** (1), 71–86.

KINOSHITA, C.M., TENG, H. & MASUTANI, S.M. 1994 A study of the instability of liquid jets and comparison with Tomotika's analysis. *Intl J. Multiphase Flow* **20** (3), 523–533.

KOROVIN, V.M. 2001 The capillary instability of a thin cylinder of viscous ferrofluid in a longitudinal magnetic field. *Z. Angew. Math. Mech.* **65** (2), 243–251.

KOROVIN, V.M. 2002 Capillary disintegration of a suspended filamentary drop of a viscous magnetic fluid in a longitudinal magnetic field. *Tech. Phys.* **47** (10), 1226–1236.

KOROVIN, V.M. 2004 Capillary disintegration of a configuration formed by two viscous ferrofluids surrounding a current-carrying conductor and having a cylindrical interface. *Tech. Phys.* **49** (6), 669–676.

KOROVIN, V.M. 2020 Capillary instability of a cylindrical ferrofluid jet in a uniform longitudinal magnetic field. *Tech. Phys.* **65** (5), 691–695.

LUCK, R., ZDANIUK, G.J. & CHO, H. 2015 An efficient method to find solutions for transcendental equations with several roots. *Intl J. Engng Maths* **2015**, 1–4.

MIKAMI, T., COX, R.G. & MASON, S.G. 1975 Breakup of extending liquid threads. *Intl J. Multiphase Flow* **2** (2), 113–138.

PATRASCU, C. & BALAN, C. 2018 Temporal instability of a viscoelastic liquid thread in the presence of a surrounding viscoelastic fluid. *J. Non-Newtonian Fluid Mech.* **261**, 164–170.

STONE, H.A. & BRENNER, M.P. 1996 Note on the capillary thread instability for fluids of equal viscosities. *J. Fluid Mech.* **318**, 373–374.

TOMOTIKA, S. 1935 On the instability of a cylindrical thread of a viscous liquid surrounded by another viscous fluid. *Proc. R. Soc. Lond.* A **150** (870), 322–337.

TOMOTIKA, S. 1936 Breaking up of a drop of viscous liquid immersed in another viscous fluid which is extending at a uniform rate. *Proc. R. Soc. Lond.* A **153** (879), 302–318.